

# 行政院國家科學委員會專題研究計畫成果報告

## 船舶操控之非線性強健控制研究

### The Nonlinear H-infinity Control of Ship Maneuvering

計畫編號：NSC-91-2213-E-164-001

執行期限：91年1月1日至91年7月31日

主持人：楊伯華 修平技術學院機械工程學系

計畫參與人員：陳清祺 修平技術學院電機工程學系

#### 中文摘要

本計畫提出非線性強健控制之設計方法，並應用於船舶操控問題。首先，探討船舶開迴路之操縱性能，如航行轉圈及 Z 形連續轉彎等。隨後藉由提出之非線性強健控制設計法，其中內迴路係運用  $H_\infty$  輸入／輸出線性化求解非線性  $H_\infty$  控制器，在外迴路設計  $\mu$ -合成強健控制器以求解船舶操縱問題。本計畫並附上系統模擬，包括船舶操控之航向保持、轉彎及追跡問題，以驗證非線性  $H_\infty$  控制之優越性能。

關鍵詞：非線性  $H_\infty$  控制、船舶操縱控制、 $H_\infty$  輸入／輸出線性化、 $\mu$ -合成

#### Abstract

In this project, the design procedure of the robust nonlinear controller is introduced and applied to the ship maneuvering problem. First, the open-loop ship maneuvering performances, such as turning circle and zig-zag maneuver, are investigated. Then the robust nonlinear controller, with the inner-loop nonlinear  $H_\infty$  controller design by the  $H_\infty$  I/O linearization and the outer-loop  $\mu$ -synthesis robust controller, is proposed to design the ship maneuvering controller. The simulations of the ship maneuvering for the course-keeping, turning, and tracking problems are enclosed to demonstrate the superiority of the nonlinear  $H_\infty$  controller.

Keywords: nonlinear  $H_\infty$  control, ship maneuvering control,  $H_\infty$  I/O linearization,  $\mu$ -synthesis

#### 1. Introduction

As the linear  $H_\infty$  control theory [1-4] has been developed for years, the controller designed based on this theory can provide the plant to reduce the disturbance from the environment and the closed-loop system can achieve the performance as expected. Recently, a much more complicated nonlinear  $H_\infty$

problem has also been solved by the concept of energy dissipation approach [5-8]. The construction of the controller and the necessary and sufficient conditions had been derived [5]. Due to the complication of operating a ship and the uncertainty disturbance from the environment, the maneuvering problem of a ship can be treated as a nonlinear  $H_\infty$  problem. The maneuvering of a ship includes the following: course keeping, turning, tracking, and berthing [9-10] can be considered as a nonlinear problem. As formulated, the state parameters variation will become the uncertainty of the controlled plant. Other external uncertainty actually comes from the hydrodynamic disturbance due to the wind, wave and current. Accordingly, a ship model is described as a nonlinear uncertain controlled plant when maneuvering. Therefore, the control to the ship becomes a nonlinear robust problem. Before applying the proposed nonlinear control techniques, the open-loop ship maneuvering performances will be investigated. In the project all ship maneuvering, except some berthing maneuvers, involves turning motion, the turning circle and the zig-zag maneuver trial simulations are provided.

In this project the design procedures of the robust nonlinear control are proposed, which can be divided into two steps: the inner-loop nonlinear controller that achieves input/output (I/O) linearization and the outer-loop linear robust controller that meets the tracking, regulation, and robustness requirements [7-8]. We first choose a linear reference, in which a convenient choice is the Taylor linearization of the nonlinear system at the equilibrium point of interest. Then, a nonlinear  $H_\infty$  controller is designed to minimize the  $H_\infty$  norm of the difference between the compensated nonlinear system and the linear reference model. In the outer-loop controller design, we start by representing the inner-loop nonlinear system by the linearized model with an uncertainty characterized by the  $H_\infty$  norm. A  $\mu$ -synthesis [3-4] problem formulation is then set up to construct a linear robust controller. The overall controller is the integration of the inner-loop nonlinear controller and

the outer-loop linear robust controller. Due to the insufficient applications of nonlinear ship control are available in the literatures, the proposed design procedures will be directly employed to the ship maneuvering control problems. The evaluation of proposed nonlinear controller is based on three ship maneuvering cases: course-keeping, turning, and tracking problems and the simulations for the closed-loop system are included to demonstrate the performance of the controller.

## 2. Ship Maneuvering

In this section, the nonlinear ship model is introduced and the ship maneuvering performance trials are investigated.

### 2.1 Nonlinear Ship Model

Assume the rigid-body ship dynamics are described by the six degrees of freedom: surge, sway, heave, pitch, roll, and yaw. For simplicity, pitch and heave can be ignored due to mild sea wave environment. The ship motion reference coordinate system is shown in Fig. 1 where

- $x_a, y_a, z_a$  : direction of 3 coordinates
- $\phi, p$  : roll angle, roll rate
- $\psi, \delta$  : heading angle, rudder angle
- $u, v$  : surge velocity, sway velocity
- $r$  : yaw rate
- $U$  : instantaneous speed

The nonlinear model adopted in this project is defined as the following [8,9]:

$$\dot{x} = Ax + f_h(x) + B_2\delta \quad (1a)$$

where

$$x = [v \ p \ r \ \phi \ \psi]^T \quad (1b)$$

Assume all the states can be measured and hence the output equation can be represented by

$$y := [v \ p \ r \ \phi \ \psi]^T := C_2x \quad (2)$$

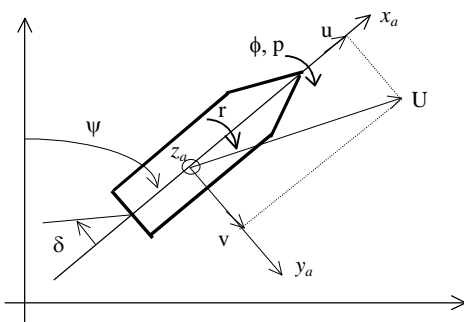


Fig. 1 Ship motion coordinate system

### 2.2 Ship Maneuvering Characteristics

In SNAME [11], there described detailed guide for sea trials for performing ship steering maneuvering. The standard ship maneuvers can be used to evaluate the robustness, controllability, performance, and limitations of the rudder steering system. Generally, the standard ship maneuvers tests include Turning Circle, Kempf's Zig-zag, Pull-out, Spiral Maneuvers, Stopping Trials, ... etc. Because these trials shall be tested in real sea environment for full-scale maneuvering trials, there are a lot of works involved and factors varying, for example, ship itself, sea wave, wind, manpower, test equipments. So, before the full-scale trials, one can perform the simulations to examine the ship's steering maneuvering characteristics. In this project, the following two trials, turning circle and Zig-zag maneuver, are simulated.

#### 2.2.1 Turning Circle

The test can be used to check the rudder's performance during course-changing (or turning) maneuver. In the trial, the ship is turned over at maximum speed, 15 knots, and with a rudder angle of 15 degrees to obtain the turning circle. Generally, the turning path of a ship is characterized by 4 numerical measures: advance, transfer, tactical diameter, and steady turning radius. Fig. 2 shows the simulation of the ship turning circle, in which the above four key measurements are also defined in the plot. From Fig. 2, we can find that the advance, transfer, tactical diameter, and steady turning radius are 862, 277, 731, and 382 meters respectively.

From some turning theories [9, 10], we know that the steady turning radius would be proportional to the ship length,  $L$ , and inversely proportional to the rudder deflection angle. A highly stable ship requires more maneuvering effort than a marginally stable one.

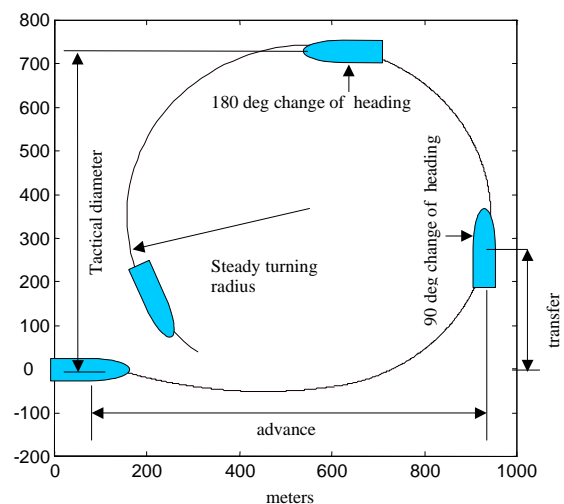


Fig. 2 Simulation of ship turning circle

#### 2.2.2 Zig-zag Maneuver

This test is also known as the overshoot maneuver. The purpose of the trial is to check the ability of the

ship's rudder to control the ship. The typical procedures for conducting the test are as follows [12]:

- (i) The ship is "steadied" on a straight course at a preselected speed, say 15 knots.
- (ii) Deflect the rudder to 10 degree, and hold until the change of the heading angle 10 degree is reached.
- (iii) At this point deflect the rudder to opposite angle of 10 degree and hold until the execute change of the heading angle 10 degrees on the opposite side is reached
- (iv) Repeat (ii) to (iii) until sufficient trial data are collected and this completes the test.

The Zig-zag Maneuver test simulation for the nonlinear ship model is shown in Fig. 3. In Fig. 3, we can see the overshoot and the period are computed as 3.4 degrees and 32.1 seconds, which can be used as an important parameter in the ship control system design [9,10].

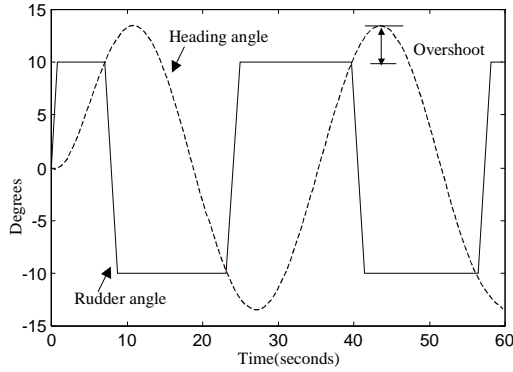


Fig. 3 Zig-zag maneuver test

### 3. Nonlinear Ship Maneuvering Control

#### 3.1 The Nonlinear $H_\infty$ Control Problem

Consider the following nonlinear input-affine generalized plant  $G$ :

$$G : \begin{cases} \dot{x} = f(x) + g_1(x)w + g_2(x)u \\ z = h_1(x) + D_{12}(x)u \\ y = h_2(x) + D_{21}(x)w \end{cases} \quad (3)$$

where  $x \in \mathbf{R}^n$  is the state of the system,  $z \in \mathbf{R}^{p_1}$  is the controlled output,  $w \in \mathbf{R}^{m_1}$  is the exogenous input including all commands and disturbances,  $u \in \mathbf{R}^{m_2}$  represents the control input, and  $y \in \mathbf{R}^{p_2}$  is the measured output. The problem is to find a nonlinear controller

$$K : \begin{cases} \dot{\xi} = A_K(\xi) + B_K(\xi)y \\ u = C_K(\xi) \end{cases} \quad (4)$$

such that the closed-loop system is stable and  $\gamma$ -dissipative [7]. The modified nonlinear  $H_\infty$  controller formulas are introduced in the following theorem [7, 13].

**Theorem 3.1** Consider the nonlinear generalized plant defined in (3) whose linearized model is in the canonical form [7, 13]. If there exists a controller  $K$  of the form (4) such that the closed-loop system is stable and  $\gamma$ -dissipative, then we have the following:

- (1) There exist  $X(x)$  and  $Y_H(x_1)$  such that the following Hamilton-Jacobi inequalities:

$$2X^T(x)H_A(x) + X^T(x)H_R(x)X(x) + H_Q(x) \leq 0 \quad (5)$$

$$2Y_H^T(x_1)J_A(x_1) + Y_H^T(x_1)J_R(x_1)Y_H(x_1) + J_Q(x_1) \leq 0 \quad (6)$$

are satisfied for all  $x$  in the domain of interest where

$$H_A(x) = f(x) - g_2(x)E_1^{-1}(x)D_{12}^T(x)h_1(x)$$

$$H_R(x) = \gamma^{-2}g_1(x)g_1^T(x) - g_2(x)E_1^{-1}(x)g_2^T(x)$$

$$H_Q(x) = h_1^T(x)h_1(x) - h_1^T(x)D_{12}(x)E_1^{-1}(x)D_{12}^T(x)h_1(x) \quad (7)$$

$$J_A(x_1) = f(x_1,0) - g_1(x_1,0)D_{21}^T(x_1,0)E_2^{-1}(x_1,0)h_2(x_1,0)$$

$$J_R(x_1) = \gamma^{-2}g_1(x_1,0)g_1^T(x_1,0) - \gamma^{-2}g_1(x_1,0)D_{21}^T(x_1,0)$$

$$J_Q(x_1) = h_1^T(x_1,0)h_1(x_1,0) - \gamma^2 h_2^T(x_1,0)E_2^{-1}(x_1,0)h_2(x_1,0) \cdot E_2^{-1}(x_1,0)D_{21}(x_1,0)g_1^T(x_1,0) \quad (8)$$

$X(x)$  can be partitioned as

$$X(x) = \begin{bmatrix} X_1(x_1, x_2) \\ X_2(x_1, x_2) \end{bmatrix} \quad (9)$$

according to the partition in [7, 13] and  $Y_H(x_1)$  has a structure as:

$$Y_H(x_1) := \begin{bmatrix} Y_{11}(x_1) \\ X_2(x_1, 0) \end{bmatrix} \quad (10)$$

- (2) The function

$$Z_1(x_1) := Y_{11}(x_1) - X_1(x_1, 0) \quad (11)$$

is the gradient of a positive function in the neighborhood of the equilibrium point.

- (3) A nonlinear  $\gamma$ -dissipative  $H_\infty$  controller can be constructed by the following formulas:

$$A_K(\xi) = f(\xi) + \gamma^{-2}[g_1(\xi) - B_K(\xi)D_{21}(\xi)]$$

$$g_1^T(\xi)X(\xi) + g_2(\xi)C_K(\xi) - B_K(\xi)h_2(\xi)$$

$$C_K(\xi) = -E_1^{-1}(\xi)[g_2^T(\xi)X(\xi) + D_{12}^T(\xi)h_1(\xi)]$$

$$B_K(\xi) = \begin{bmatrix} B_{K1}(\xi_1) \\ B_{K2}(\xi_1) \end{bmatrix} \quad (12)$$

where

$$B_{K2}(\xi_1) = g_{12}(\xi_1)D_{21}^T(\xi_1, 0)E_2^{-1}(\xi_1, 0) \quad (13a)$$

$$g_1(\xi_1, 0) := \begin{bmatrix} g_{11}(\xi_1) \\ g_{12}(\xi_1) \end{bmatrix} \quad (13b)$$

and  $B_{K1}(\xi_1)$  satisfies the following equation

$$[Y_{11}(\xi_1) - X_1(\xi_1, 0)]^T B_{K1}(\xi_1) = [\gamma^2 h_2^T(\xi_1, 0) + Y_{11}^T(\xi_1)]$$

$$g_{11}(\xi_1)D_{21}^T(\xi_1,0) + X_2^T(\xi_1,0)g_{12}(\xi_1)D_{21}^T(\xi_1,0)]E_2^{-1}(\xi_1,0)$$

### 3.2 Robust Nonlinear Controller Design

The design procedure of the proposed robust nonlinear controller can be divided into two steps: the inner-loop nonlinear  $H_\infty$  controller that achieves approximate I/O linearization, and the outer-loop linear robust controller that meets the tracking, regulation, and robustness requirements. Fig. 4 shows the block diagram of the  $H_\infty$  I/O linearization problem formulation. The objective of the problem is to find a nonlinear  $H_\infty$  controller such that the compensated nonlinear system approximates the linear reference model in I/O behavior. Due to the space limitation, the detailed procedure of the problem formulation can be referred to [7, 13].

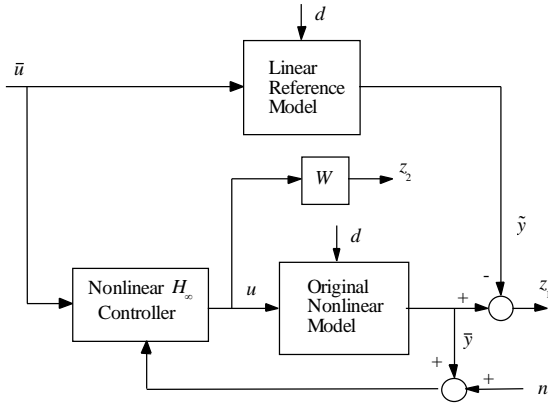


Fig. 4 The block diagram for the  $H_\infty$  I/O linearization problem

After the inner-loop controller design, the next step is to design an outer-loop linear robust controller. Fig. 5 shows the block diagram for the outer-loop controller design. The compensated inner-loop nonlinear system is represented by the linearized model and an uncertainty block  $\Delta(s)$  which is characterized by an  $H_\infty$  bound. The linear  $H_\infty$  control [1-2] and  $\mu$ -synthesis technique [3-4] can be employed to design an outer-loop linear robust controller to address the uncertainty. The structure of the overall controller will be introduced as the simulation diagram form in Section 3.4.

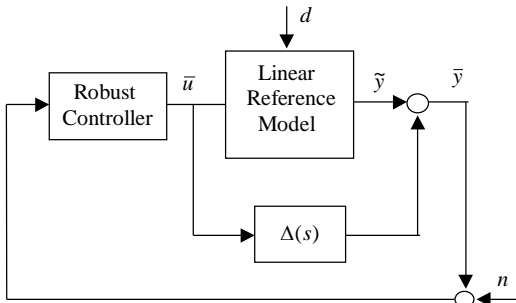


Fig. 5 Outer-loop robust controller design

### 3.3 Design Techniques Applied to Ship Maneuvering

Now, we will use the robust nonlinear control design techniques to design a maneuvering controller for the nonlinear ship model in (1,2). After applying the problem formulation of the  $H_\infty$  I/O linearization problem, one can employ the modified nonlinear  $H_\infty$  controller formulas in Theorem 3.1 and the successive algorithm for solving the Hamilton-Jacobi equations [14] to obtain the inner-loop  $H_\infty$  I/O linearization controller, although the controller is too complicated and lengthy to be included in the report.

Next, we design an outer-loop  $\mu$ -synthesis robust controller to provide robust stability/performance against the inexact dynamics matching in the inner-loop  $H_\infty$  I/O linearization design. In Fig. 6,  $P_L$  stands for the linear reference model which is the linearized model of the nonlinear plant (1-2). The objective is to find a controller  $K_\mu(s)$  so that the closed-loop system is robustly stable and the outputs of the ship controlled variables  $z$  follow  $w_t$ , the reference tracking signals, respectively as closely as possible.  $W_e$  is a weighting function for the tracking error, usually a low-pass filter; the combination of  $W_\Delta$  and  $\Delta_1$  represents the plant uncertainty, and usually  $W_\Delta$  is a high-pass filter.  $W_e$  and  $W_\Delta$  are weighting functions chosen by the designers such that the design specifications can be met. We choose them as follows.

$$W_e = \frac{0.5}{s+0.03} \quad W_\Delta = \frac{100(s+100)}{s+10000} \quad (14)$$

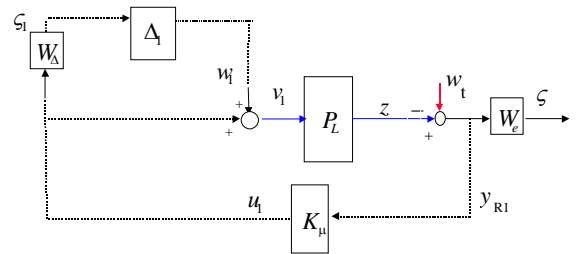


Fig. 6 Formulation of an outer-loop control problem

With the  $D$ - $K$  iteration algorithm [3-4], we first obtained an  $H_\infty$  controller  $K_1(s)$  with optimal  $H_\infty$  norm equal to 16.47 which gives the maximal singular value  $\bar{\sigma}$  plot and  $\mu$  plot of  $F_1[\hat{G}(s), K_1(s)]$  in Fig. 7, where  $F_1[G(s), K(s)]$  is the lower linear fractional transformation. Since  $K_1(s)$  ignores the structure information of  $\Delta$  and treats  $\Delta$  as a full matrix, it gives a conservative solution to the problem. From Fig. 7, we can see there exists difference between the

$\bar{\sigma}$  plot and  $\mu$  plot which means the D-K iteration can be further proceeded to reduce the  $H_\infty$  norm of the closed-loop system to obtain a better controller performance. After two iterations, the process converges to a controller  $K_2(s)$  with optimal  $H_\infty$  norm reduced to 15.85 which gives the  $\bar{\sigma}$  plot and  $\mu$  plot of  $F_1[\hat{G}(s), K_2(s)]$  in Fig. 8, where the two plots are matched together revealing that the  $H_\infty$  norm of the closed-loop system can not be further reduced, hence the D-K iteration is stopped here.

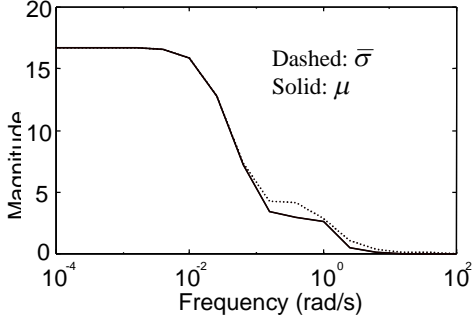


Fig. 7  $\bar{\sigma}$  and  $\mu$  plots for the 1st D-K iteration

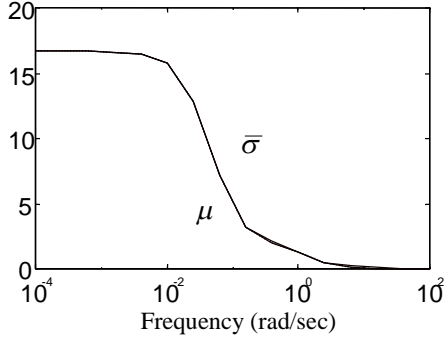


Fig. 8  $\bar{\sigma}$  and  $\mu$  plots for the 2nd D-K iteration

### 3.4 Ship Maneuvering Simulations

Time response simulations for the closed-loop system with the nonlinear inner-loop controller and the  $\mu$ -synthesis controller will be given in the following for three ship maneuvering cases: course-keeping, turning, and tracking problems. The simulation diagram of the robust nonlinear controller design is shown in Fig. 9.

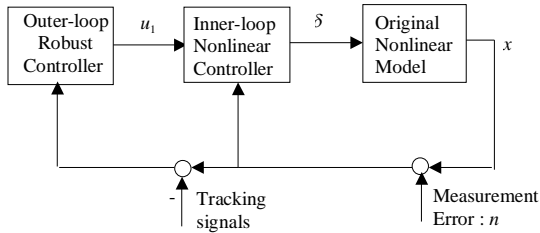


Fig. 9 Simulation diagram of the robust nonlinear controller design

#### 3.4.1 Course-keeping Problem

Now the computer simulations for the closed-loop system of the ship motion will be performed. Let the initial conditions be  $[0 \ 0 \ 0 \ 0]^T$  in which the assumption of the initial condition for the heading angle  $\psi$  is zero. It is reasonable because any desired angle is just a linear coordinate shift, for example, we can define  $\psi_{new} = \psi - \psi_d$  where  $\psi_d$  is the desired heading angle. For simplifying purpose, the exogenous input (disturbances) to the nonlinear model of the ship motion is defined as

$$d = 0.01 \sin(t) [1 - e^{-2t}] [1 \ 1 \ 1 \ 1]^T \quad (15)$$

to simulate the influence of the see wave. Note that the amplitude is very high to emphasis the performance and the robustness of the robust nonlinear controller. The measurement noise is assumed as  $n=0.001 \sin(100t)$ . The ship motion responses of the closed-loop system are plotted in Figure 10. In Figure 10, the heading angle  $\psi$  converges to 0 as desired while other states also approach to 0 which indicates the robust nonlinear works properly for the ship course-keeping problem because of providing system performance and robustness to the closed-loop system.

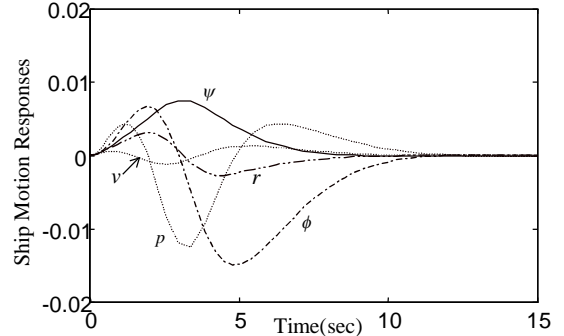


Fig. 10 Ship motion responses for course-keeping

#### 3.4.2 Turning Problem

The turning problem is also known as the course-changing problem. Consider the ship motion has a command for turning 0.2 radian then turning back to 0 degree after 25 seconds. Let the tracking signals be

$$\psi_s = \begin{cases} 0.2(1 - e^{-t}) & , 0 \leq t < 25 \\ 0.2e^{-(t-25)} & , 25 < t \end{cases} \quad (16)$$

other states = 0

The tracking signal of the heading angle  $\psi$  can be regarded as a combination of low frequency signals or as the output of the low-pass filter  $1/(s+1)$  driven by a step function, than driven back to 0 after 25 seconds, which is indicated as the dashed line in Fig. 11. Fig. 11 shows the ship turning response of the

closed-loop system. We found that the robust nonlinear controller has the performance to make the output time response follows the tracking signal.

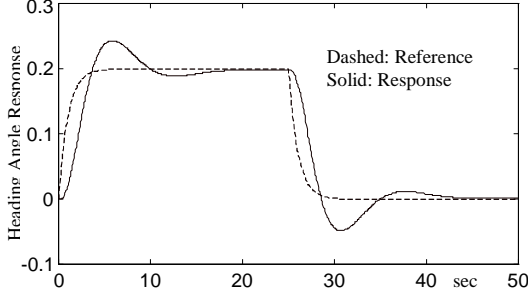


Fig. 11 Ship heading angle response for turning

### 3.4.3 Tracking Problem

Two approaches of the way point guidance tracking problem are introduced and the simulations are compared in the following [9, 10]:

- A. Way point guidance by straight line between two points

Assume that the ship is moving with forward speed  $U$ , say 10 knots, and the two way points are with the coordinates from  $[x_d(t_0), y_d(t_0)]$  to  $[x_d(t_f), y_d(t_f)]$ . The desired heading angle based on the guidance system of the straight line between the two points is computed as

$$\psi_d = \tan^{-1} \left( \frac{y_d(t_f) - y_d(t_0)}{x_d(t_f) - x_d(t_0)} \right) \quad (17)$$

The simulation of the ship maneuvering for the tracking problem based on the straight line approach is shown in Fig. 12. In Fig. 12, we can see that the desired heading angle is only changed at each way point, and hence some overshoot is as expected. Another approach is introduced as follows to resolve the overshoot problem.

- B. Way point guidance by line of sight (LOS)

Let the tracking problem be given by a set of way points  $[x_d(k), y_d(k)]$  for  $k=1, 2, \dots, N$ . The desired heading angle based on the guidance system of the line of sight is defined as

$$\psi_d(t) = \tan^{-1} \left( \frac{y_d(k) - y_d(t)}{x_d(k) - x_d(t)} \right) \quad (18)$$

If the ship location  $[x(t), y(t)]$  at the time  $t$  satisfying

$$[x_d(k) - x(t)]^2 + [y_d(k) - y(t)]^2 \leq \rho_0^2 \quad (19)$$

then the next way point  $[x_d(k+1), y_d(k+1)]$  should be selected where  $\rho_0$  is defined as the radius of the acceptance circle. The simulation of the ship maneuvering for the tracking problem based on the line of sight approach is shown in Fig. 13 where the acceptance

radius is chosen as  $\rho_0 = 0.5L$  and  $L$  denotes for ship length. In Fig. 13, we can see that there is almost no overshoot for the tracking path, although the ship does not pass exactly all the way points.

From the above observations, we know that for the two approaches, the overshoot happened and the way points passed through is a trade-off problem and can be negotiated according to the tracking mission.

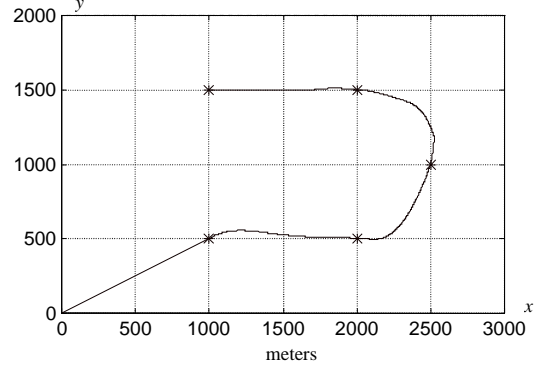


Fig. 12 Way point guidance by straight line between two points

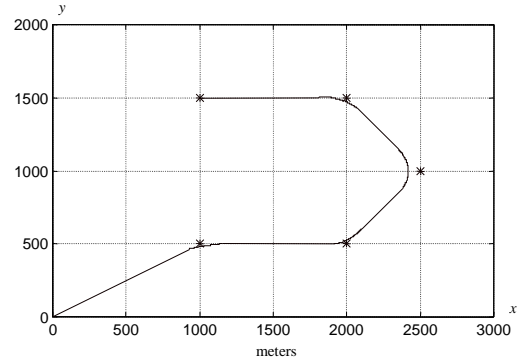


Fig. 13 Way point guidance by line of sight

## 4. Conclusions

In this project, the nonlinear ship maneuvering control problem is investigated. By the inner-loop  $H_\infty$  I/O linearization and outer-loop  $\mu$ -synthesis robust controller design, the robust nonlinear control techniques can be applied to ship maneuvering problem. The course-keeping, turning, and tracking problems are considered and the simulations show that the proposed robust nonlinear controller can provide robust stability and performance.

## 5. References

- [1] Doyle, J. C., Glover, K., Khargonekar, P. P., and Francis, B. A., "State Space Solutions to Standard  $H_2$  and  $H_\infty$  Control Problems," *IEEE Trans. on Automatic Control*, Vol.34, pp. 831-846 (1989).

- [2] Glover, K., and Doyle, J. C., "State-space Formula for All Stabilizing Controllers that Satisfy an  $H_\infty$  -norm Bound and Relations," *Systems & Control Letters*, Vol. 11, pp. 167-172 (1988).
- [3] Zhou, K., Doyle, J. C., and Glover, K., *Robust and Optimal Control*, Prentice-Hall, Inc., pp. 271-300 (1997).
- [4] Balas, G. J., Doyle, J. C., Glover, K., Packard, A., and Smith, R.,  $\mu$ -*Analysis and Synthesis Toolbox*, The Mathworks, Inc., MA, MUSYN Inc., MN., pp. 1-1~2-35 (1993)
- [5] Ball, J.A., Helton, J.W. and Walker, M.L., "  $H_\infty$  Control for nonlinear systems with output feedback," *IEEE Trans. Automat. Contr.* Vol. 38, pp. 546-559 (1993).
- [6] Van der Schaft, A.J.,  $L_2$  -Gain and Passivity Techniques in Nonlinear Control, Springer, London (1996).
- [7] Hu, S.S., Chang, B.C., Yeh, H.H., and Kwatny, H.G., "Robust Nonlinear Control Design for a Longitudinal Flight Control Problem," *Asian J. of Control*, Vol. 2, No. 2, pp. 111-121 (2000).
- [8] Hu, S. S., Yang, P. H., Su, C. M., and Juang, J. Y., "Robust Nonlinear Control Theory Applied to Ship Control," *2001 Chinese Automatic Control Conference*, pp. 471-476, Taiwan (2001).
- [9] Fossen, Thor I., *Guidance and Control of Ocean Vehicles*, John Wiley and Sons, (1998).
- [10] Crane, C.L., Eda, H., and Landsburg A., Controllability, Chapter 9, Principles of Naval Architecture.
- [11] SNAME, Guide for Sea Trials, Technical and Research Bulletin, No. 3-47, *The Society of Naval Architects and Marine Engineers*, (1989).
- [12] Gertler, M. "Steering and Maneuvering; the state of the art", *14<sup>th</sup> ATTC Conference*, Sept., (1959).
- [13] Hu, S. S., Yang, P. H., and Chang, B. C., "Modified Nonlinear  $H_\infty$  Controller Formulas and the  $H_\infty$  I/O Linearization Problem", *Proceedings of the 1998 IEEE Conference on Decision and Control* (1998).
- [14] Hu, S. S., Yang, P. H., and Chang, B. C., " On a Computational algorithm to the HJE in Nonlinear  $H_\infty$  Control," *J. of Marine Science and Technology*, Vol. 9, No. 2, pp. 91-99, Nov. (2001).

